Journal of Evolutionary Biology, 2024, **37**, 795–806
https://doi.org/10.1093/jeb/voae053
Advance access publication 3 May 2024
Research Article

JOURNAL OF
Evolutionary Biology

eseb
European Society for Evolutionary Biology

High parasite diversity maintained after an alga–virus coevolutionary arms race

Eva J.P. Lievens[1,†], Samuel Kühn[1,†], Elena L. Horas[1], Guénolé Le Pennec[2], Sarah Peter[1], Azade D. Petrosky[1], Sven Künzel[3], Philine G.D. Feulner[2,4], Lutz Becks[1]

[1]Aquatic Ecology and Evolution Group, Department of Biology, University of Konstanz, Konstanz, Germany
[2]Department of Fish Ecology and Evolution, EAWAG, Swiss Federal Institute of Aquatic Science and Technology, Kastanienbaum, Switzerland
[3]Department of Evolutionary Genetics, Max Planck Institute for Evolutionary Biology, Plön, Germany
[4]Department of Biology, Institute of Ecology and Evolution, University of Bern, Bern, Switzerland

Corresponding author: Eva J.P. Lievens, Aquatic Ecology and Evolution Group, Department of Biology, University of Konstanz, Universitätsstraße 10, 78464 Konstanz, Germany. Email: eva.j.lievens@gmail.com
[†]Equal contribution.

Abstract

Arms race dynamics are a common outcome of host–parasite coevolution. While they can theoretically be maintained indefinitely, realistic arms races are expected to be finite. Once an arms race has ended, for example due to the evolution of a generalist-resistant host, the system may transition into coevolutionary dynamics that favour long-term diversity. In microbial experiments, host–parasite arms races often transition into a stable coexistence of generalist-resistant hosts, (semi-)susceptible hosts, and parasites. While long-term host diversity is implicit in these cases, parasite diversity is usually overlooked. In this study, we examined parasite diversity after the end of an experimental arms race between a unicellular alga (*Chlorella variabilis*) and its lytic virus (PBCV-1). First, we isolated virus genotypes from multiple time points from two replicate microcosms. A time-shift experiment confirmed that the virus isolates had escalating host ranges, i.e., that arms races had occurred. We then examined the phenotypic and genetic diversity of virus isolates from the post-arms race phase. Post-arms race virus isolates had diverse host ranges, survival probabilities, and growth rates; they also clustered into distinct genetic groups. Importantly, host range diversity was maintained throughout the post-arms race phase, and the frequency of host range phenotypes fluctuated over time. We hypothesize that this dynamic polymorphism was maintained by a combination of fluctuating selection and demographic stochasticity. Together with previous work in prokaryotic systems, our results link experimental observations of arms races to natural observations of long-term host and parasite diversity.

Keywords: *Chlorella variabilis*, PBCV-1, host–parasite coevolution, arms race dynamics, fluctuating selection, diversity, time-shift experiment, host range, resistance

Introduction

Host–parasite coevolution is regarded as an important driver of diversity because it can generate and maintain polymorphisms in host resistance and parasite host range (Buckingham & Ashby, 2022; Clarke, 1979). Reciprocal selection between hosts and parasites can take various forms, including fluctuating selection, selection for static mono- or polymorphisms, and directional selection (reviewed in Agrawal & Lively, 2002; Best et al., 2017; Buckingham & Ashby, 2022; Woolhouse et al., 2002). Fluctuating selection acts on qualitative or quantitative differences in resistance or host range (e.g., matching alleles models, gene-for-gene and continuous range models with costs), producing dynamic polymorphisms that can maintain diversity indefinitely ("coevolutionary cycles," Best et al., 2017). Long-term diversity can also be maintained by selection for static polymorphisms of resistance and host range. In contrast, directional selection for escalating resistance and host range produces infinite arms race dynamics (e.g., gene-for-gene and continuous range models without costs). Infinite arms races preclude diversity, but are not ecologically realistic: if mutational limitations or costs of resistance/host range occur, arms race dynamics are expected to be transient (Best et al., 2017; Brown & Tellier, 2011; Buckingham & Ashby, 2022; Lenski, 1984).

Arms race dynamics are a common outcome of experimental coevolution, particularly in microbial systems under permissive conditions (Brockhurst et al., 2003; Chao et al., 1977; Common et al., 2019; Frickel et al., 2016; Gómez et al., 2015; Hall et al., 2011; Kashiwagi & Yomo, 2011; Larsen et al., 2019; Lenski & Levin, 1985; Lopez Pascua et al., 2014; Marston et al., 2012; Mizoguchi et al., 2003; Perry et al., 2015; Retel et al., 2019). Microbial arms races are often finite, ending when a generalist-resistant host phenotype evolves (a host phenotype that resists infection by parasites from all time points). The evolution of a generalist-resistant host can drive the parasite extinct (Common et al., 2019). More commonly, however, the system transitions into a stable coexistence of parasites, generalist-resistant hosts, and susceptible or "semi-" susceptible hosts (host phenotypes that resist infection by parasites from, respectively, zero or some time points) (Chao et al., 1977; Frickel et al., 2016; Hall et al., 2011; Horas, 2022; Lenski & Levin, 1985; Lopez Pascua et al., 2014; Marston et al., 2012; Retel et al., 2019). In other words, many microbial arms races transition into post-arms

Received October 1, 2023; revised February 27, 2024; accepted May 2, 2024
© The Author(s) 2024. Published by Oxford University Press on behalf of the European Society of Evolutionary Biology.
This is an Open Access article distributed under the terms of the Creative Commons Attribution License (https://creativecommons.org/licenses/by/4.0/), which permits unrestricted reuse, distribution, and reproduction in any medium, provided the original work is properly cited.

Downloaded from https://academic.oup.com/jeb/article/37/7/795/7663659 by Lib4RI - Library of Eawag, Empa, PSI, WSL user on 07 October 2024

race dynamics that maintain host diversity (typically because resistance trades off with growth, Chao et al., 1977; Frickel et al., 2016; Lenski & Levin, 1985; Retel et al., 2019). Whether these post-arms race dynamics also maintain parasite diversity is much less well-studied (Chao et al., 1977; Hall et al., 2011; Lopez Pascua et al., 2014; Marston et al., 2012). Since stable coexistence is likely to be more representative of natural host–parasite communities (Brown & Tellier, 2011; Flores et al., 2011; Poisot et al., 2013), understanding when and how parasite diversity is maintained will help link laboratory experiments to natural observations.

In this study, we examined the maintenance of parasite diversity after a coevolutionary arms race between a unicellular alga, *Chlorella variabilis*, and its lytic virus, PBCV-1 (Van Etten et al., 2020). Coevolutionary dynamics in this system typically follow an arms race with three rounds of algal resistance evolution and two rounds of viral host range evolution (Frickel et al., 2016; Horas, 2022; Retel et al., 2019). The arms race ends with the evolution of a generalist-resistant algal phenotype, but post-arms race algal polymorphism—and thus viral replication—is maintained by a trade-off between algal resistance and growth rate (Frickel et al., 2016; Horas, 2022; Retel et al., 2019). As yet, nothing is known about the virus' phenotypic diversity during the post-arms race phase. To address this, we isolated virus genotypes from multiple time points of a previous coevolution experiment and studied their phenotypic and genetic diversity.

Methods

Background

This study is based on an alga–virus coevolution experiment described in Horas (2022). Experimental microcosms were inoculated with single clones of *C. variabilis* and PBCV-1 and tracked for 90 days. Microcosms were shaken continuously to avoid environmental heterogeneity. Each day, 10% of the volume was removed and replaced with fresh medium. The removed volume was used to measure the density of algae and viruses, to store a sample of the virus population (the free-living virus particles, stored at 4 °C), and to store a sample of the algal clones (stored as colonies on agar plates). The stored samples were later used to perform time-shift experiments: algal clones from ~18 time points were tested for their ability to resist infection by virus populations from the same time points. The time-shift experiments provided measures of both algal resistance (the proportion of virus populations that an algal clone could resist) and viral host clone range (the proportion of algal clones that a virus population could infect). Three of four replicate microcosms demonstrated transient arms race dynamics.

We focused on two microcosms with similar dynamics (Figure 1A and B). The arms race dynamics are visible as increases in algal resistance (detected on days 16, 43, and 67 in microcosm I; on days 16, 43, and 62 in microcosm II) and viral host clone range (detected on days 29 and 67 in microcosm I; on days 25 and 53 in microcosm II). The arms race ended once generalist-resistant algae evolved (detected on day 67 in microcosm I; on day 62 in microcosm II). The "post-arms race" phase, i.e., the phase characterized by the presence of generalist-resistant algae, continued until the end of the experiment. Generalist resistance was the dominant algal phenotype during this phase, but viral replication continued (Supplementary Figure S1). We therefore assume that (semi-)susceptible algae occurred at low frequencies, as found in previous work (Frickel et al., 2016; Retel et al., 2019).

Virus isolation

In order to study viral diversity, we isolated single virus genotypes from the populations collected by Horas (2022). Hereafter, we use "virus isolate" to describe a virus suspension amplified from a single infectious virion. Virus isolates consist of a single genotype, which may or may not be shared with other virus isolates. "Virus" is used as a general term; "virion" refers to free-living virus particles; "infectious virions" refers to virions that are capable of lysing a host cell and releasing progeny, i.e., capable of catalyzing the death of an algal culture (Van Etten et al., 1983b).

For each microcosm, we isolated viruses from the virus populations sampled from the coevolution experiment on days 34, 43, 53, 62, 67, and 85. To maximize the diversity of the virus isolates, we used different algal clones as isolation environments (the "isolation algae," Figure 1A and B). Each virus population could infect between 2 and 12 isolation algae; we collected one virus isolate per infectious combination (dots in Figure 1A and B). Isolations were done using plaque or dilution methods. The isolation method did not affect the phenotypes or genotypes of the virus isolates (data not shown). Plaque-based isolations were performed following Van Etten et al. (1983a): virus populations were diluted and plated onto a lawn formed by the isolation alga, and individual plaques were amplified in the same alga. Dilution-based isolations were done in two steps: first, we used "most probable number" assays to measure the concentration of virions in a virus population that were infectious to an isolation alga (Zimmerman, 2017); second, we aliquoted the virus population into 96 liquid culture wells of that alga such that each well received 0.05 infectious virions. After incubation, wells were identified as virus-positive (lysed) or virus-negative. Assuming 0.05 infectious virions per well, the probability that a virus-positive well was inoculated with a single infectious virion was 0.975; allowing for errors in the MPN measurement, the probability was > 0.9. One virus-positive well was then amplified in the same isolation alga. For both the plaque and dilution methods, amplified virus isolates were filtered through 0.45 µm and stored at 4 °C. Their virion concentration was measured by flow cytometry (on protocols.io: Lievens, 2022; Lievens et al., 2023).

Arms race confirmation

The time-shift experiment done by Horas was performed at the virus population level (Figure 1A and B). As in previous studies, it was assumed that broad host clone ranges at the population level reflected the evolution of broad host clone range genotypes, i.e., reflected an arms race (Frickel et al., 2016; Retel et al., 2019). However, it was also possible that virus populations contained multiple genotypes with complementary narrow host clone ranges. To confirm that arms race dynamics had occurred, we performed an isolate-level time-shift experiment using the isolation algae and virus isolates (cf. Buckling & Rainey, 2002; Hall et al., 2011; Lopez Pascua et al., 2014). For each isolation alga × virus isolate combination, we inoculated four liquid culture wells with 2×10^4 virions/ml and 2×10^5 algae/ml, to a final volume of 0.2 ml (multiplicity of particles 0.1). The cultures were incubated for 10 days, and the optical density at 680 nm was measured every second day. We identified wells as virus-positive (lysed)

Downloaded from https://academic.oup.com/jeb/article/37/7/795/7663659 by Lib4RI - Library of Eawag, Empa, PSI, WSL user on 07 October 2024

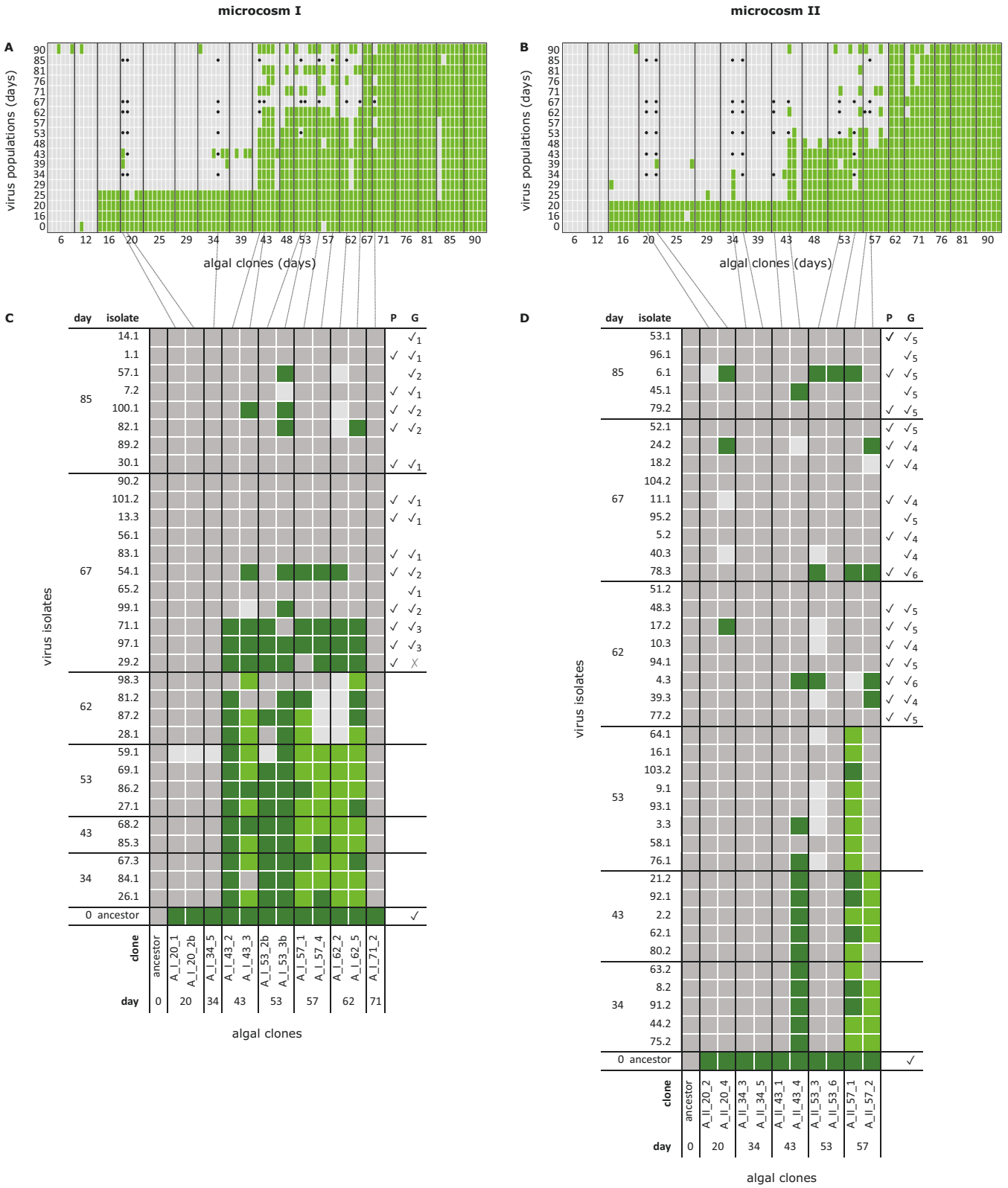


Figure 1. Population- and genotype-level arms race dynamics in alga–virus coevolution. (A and B) Infection matrices for the time-shift experiment performed by Horas (2022) (reproduced with permission). Algal clones (columns) were tested for their ability to resist virus populations (rows), and classed as resistant (light green) or susceptible (light grey). A subset of the algal clones was used as environments to isolate virus genotypes ("isolation algae"); virus population × isolation alga combinations that were used to produce a virus isolate are marked with a black dot. (C and D) Infection matrices for the time-shift experiment confirming arms race dynamics. The isolation algae and ancestor alga (columns) were tested for their ability to resist virus isolates and the ancestor virus (rows), and classed as resistant (dark green) or susceptible (dark grey). If the combination could not be tested, the population-level result is shown (resistant: light green; susceptible: light grey). Selected virus isolates from the post-arms race phase were used to obtain additional phenotypic (✓ under "P") or genetic information (✓ under "G" if successful, × if not). Where relevant, the assignment of genetic cluster is appended (e.g., $✓_1$ for genetic cluster 1; see text). Names of the virus isolates are abbreviated from, e.g., "PBCV-1-H-13.3" to "13.3."

Downloaded from https://academic.oup.com/jeb/article/37/7/795/7663659 by Lib4RI - Library of Eawag, Empa, PSI, WSL user on 07 October 2024

or virus-negative using longitudinal *k*-means clustering of the optical densities (package "kml," Genolini et al., 2015) in R (R Core Team, 2020). Isolation alga × virus isolate combinations were classed as susceptible if at least three of four replicates were virus-positive (grey in Figure 1C and D), and as resistant if at least three of four replicates were virus-negative (green in Figure 1C and D). Some combinations could not be completed due to the loss of algal clones over time (light grey or light green in Figure 1C and D).

Diversity in the post-arms race phase

We assessed the phenotypic and genetic diversity of viruses in the post-arms race phase using virus isolates from the beginning and end of the phase. For microcosm I, these were isolates from, respectively, day 67 (n = 11 isolates) and day 85 (n = 8 isolates). For microcosm II, we used isolates from, respectively, days 62 and 67 (n = 8 and 9 isolates) and day 85 (n = 5 isolates) (Figure 1C and D).

Phenotypic diversity

We measured the virus isolates' key life history phenotypes: host clone range, survival in the environment, and growth rate in the host. The host clone range was measured for all of the available isolates. Survival and growth rate were measured in a subset of the isolates (marked under "P" in Figure 1C and D), after re-amplification in the ancestor alga. For re-amplification, ancestor algal cultures (10 ml, 1 × 10^6 algae/ml) were inoculated with a modest number of viruses, incubated until lysis was visible (1–2 days), and filtered through 0.2 µm to remove algae and bacteria. Amplified isolates were stored at 4 °C, and the concentration of virions was measured by flow cytometry (on protocols.io: Lievens, 2022; Lievens et al., 2023).

Host clone range was measured by the isolate-level time-shift experiment described above, and expressed as the proportion of isolation algae + ancestor alga that the virus isolate could infect (cf. Figure 1C and D). A host clone range of 1.0 indicates that a virus could infect all of the isolation algae from its own microcosm. Note that the isolation algae did not include any generalist-resistant phenotypes, so a host clone range of 1.0 does not mean that a virus could infect generalist-resistant algae.

To quantify survival, we measured the proportion of infectious virions that survived 7 days of exposure to the environmental conditions used in the coevolution experiment (constant white light at 50 µmol m^{-2} s^{-1}, 20 °C), following the "modified survival assay" described in Lievens et al. (2023) (on protocols.io: Lievens, 2023). Briefly, we prepared viral suspensions with a 10,000-fold range of initial virion concentrations. Before and after exposure to the environment, aliquots of these suspensions were distributed across 16 liquid culture wells of the ancestor alga. The cultures were incubated for 4 days, after which the wells were classed as virus-positive (lysed) or virus-negative based on their optical density at 680 and 750 nm using Gaussian mixture modelling (package "mclust," Scrucca et al., 2016) in R (R Core Team, 2020). (For experiments with a large number of wells and comparable data, i.e., a single algal clone at a single time point, Gaussian mixture models are more sensitive than the *k*-means clustering used above.) The assay was replicated twice. For each virus isolate, the numbers of virus-positive and -negative wells were used as binomial response variables in generalized non-linear mixed models, with replicate included as a random effect (in R, R Core Team, 2020; package "repeated," Swihart & Lindsey, 2022). The models estimated the initial concentration of infectious virions and the proportion of infectious virions that survived until day 7.

The virus isolates' growth rate was measured in the ancestor alga. We inoculated liquid culture wells with 2.5 × 10^4 virions/ml and 1 × 10^6 algae/ml, to a final volume of 0.2 ml (multiplicity of particles 0.025). The infections were incubated for 24 hr. The wells were then centrifuged for 15 min at 2,000 g to separate algae and viruses, and supernatants were stored at 4 °C. The virion concentration of the supernatants was measured by flow cytometry (on protocols.io: Lievens, 2022; Lievens et al., 2023). We calculated the growth rate as *ln*(final virion concentration/initial virion concentration)/24 hr. Each isolate was replicated twice.

Afterwards, we tested for pairwise correlations between the three phenotypes using Spearman's rank method. Correlations were tested within each microcosm and corrected for multiple testing using Holm's method (Holm, 1979).

Genetic diversity

We investigated the genetic diversity of post-arms race viruses using a subset of the virus isolates (marked under "G" in Figure 1C and D). These virus isolates were processed together with several viruses isolated from the arms race phase, whose results are not included in this study. To obtain enough viral DNA, we amplified each isolate in the ancestor alga. Ancestor algal cultures (100 ml, 1–4*10^6 algae/ml) were inoculated with a modest number of viruses and incubated until lysis was visible (1–3 days). Algae and bacteria were removed from the lysed cultures by centrifuging for 30 min at 3,000 g and filtering the supernatants through 0.2 µm. The virions were then collected onto a 0.1 µm filter, and DNA was extracted from the filter using a Qiagen DNeasy PowerWater kit (QIAGEN GmbH, Germany). Libraries were prepared analogously to Illumina Nextera Flex kits (Picelli et al., 2014) and sequenced on an Illumina MiSeq system (paired-end 2 × 150 bp, Illumina, USA). The ancestor virus and virus isolate PBCV-1-H-79.2 were extracted and sequenced twice as a quality control measure. Reads were pre-processed in fastp v. 0.20.0 (Chen et al., 2018). This consisted of trimming Illumina adapter sequences and polyG tails (default settings), and merging forward and reverse reads in case they overlapped (with the settings overlap_len_require set to 20, overlap_diff_limit set to 5, and overlap_diff_percent_limit set to 5). We also trimmed 3′ end tails of reads if the mean quality dropped below 15 and removed reads shorter than 70 bases. Reads of all virus isolates, including the ancestor virus, were mapped onto the PBCV-1 reference genome (NCBI GenBank, accession: NC_000852.5) using bwa v.0.7.17 (Li & Durbin, 2009). The alignment files were then processed using tools in GATK v. 4.2.2.0 (Van der Auwera & O'Connor, 2020). We first applied FixMateInformation to all bam files, then merged paired-end and single-end bam files per sample with MergeSameFiles, and marked duplicate reads with MarkDuplicateSpark. The resulting bam files had an average depth of coverage of 63 × (Supplementary Table S1). Coverage was homogenous across the genome (standard deviation 23 ×), with only 100 sites with no coverage (0.03% of the genome) and 25,964 sites with an average coverage below 10 × (8% of the genome).

We processed the viral sequences following two independent pipelines. First, genetic variation was called separately on

Downloaded from https://academic.oup.com/jeb/article/37/7/795/7663659 by Lib4RI - Library of Eawag, Empa, PSI, WSL user on 07 October 2024

all bam files using GATK's HaplotypeCaller, with minimum mapping quality set to 20 and a minimum base quality score of 10. The parameter -ploidy was set to 1 since isolates were expected to be single genotypes, and the option -ERC was set to output GVCF format. The resulting GVCFs were combined in a single-cohort VCF with GATK's CombineGVCFs, and genotypes were called on this cohort with GATK's GenotypeGVCFs (with -sample-ploidy set to 1). The resulting VCF file contained 88 sites. In order to minimize sequencing artefacts and misalignments, we applied a stringent filtering strategy that removed all sites with ambiguous calls among technical replicates (ancestor virus and PBCV-1-H-79.2, see above). We used vcftools v. 0.1.15 (Danecek et al., 2011) to remove indels and sites with more than two alleles. The resulting VCF file contained 35 SNPs. SNP genotypes were extracted with a bash script, and loci with more than 20% missing genotypes were removed. This gave a final number of 24 SNPs compared to the PBCV-1 reference genome, of which 19 occurred in the ancestor or post-arms race viruses (Supplementary Table S1). SNP coding effects were classified by SnpEff v5.1d (Cingolani et al., 2012; Supplementary Table S2). Second, we looked for copy number variation along the genome. We used germline tools, which are well-suited to haploid data, in GATK-4.2.2.0 (Van der Auwera & O'Connor, 2020). The PBCV-1 reference genome was divided into 1 kb intervals using PreprocessIntervals (default settings), and read counts were collected for every interval using CollectReadCounts (-interval-merging-rule set to overlapping only). We applied DetermineGermlineContigPloidy to the read counts to determine the baseline copy number for each virus isolate (contig ploidy priors: 97% for ploidy 1, 1% for ploidies 0, 2, and 3), and GermlineCNVCaller to obtain posterior probabilities and copy number variation calls. PostprocessGermlineCNVCalls was then used to generate genotype intervals and genotyped segments in VCF formats (-autosomal-ref-copy-number set to 1). This pipeline identified five copy number variations in the ancestor or post-arms race viruses compared to the PBCV-1 reference genome (Supplementary Table S1). The patterns were consistent with two distinct deletions having occurred during the experimental coevolution: when compared to the ancestor virus, all post-arms race isolates had a large deletion between 15 and 41 kb or 16 and 41 kb (each associated with the deletion of specific ancestral duplications, Supplementary Table S1). There were no filtered SNPs in any of the duplicated or deleted regions.

After genotyping, we grouped the virus isolates into genetic clusters based on their differences from the ancestor virus. We coded the genotypes of the virus isolates as identical to (0) or different from (1) the ancestor virus at each of the 19 SNPs that occurred in these viruses, and recorded whether each isolate had (1) or did not have (0) one of the two large deletions. The distance between isolates was calculated using Gower's general dissimilarity coefficient for asymmetric binary variables, and clustering was done using a *k*-medoids approach (Gower, 1971; Kaufman & Rousseeuw, 1990). These analyses were done in R using the "cluster" package; the optimal cluster number was found using the "kneedle" algorithm (Maechler et al., 2022; R Core Team, 2020; Tam, 2022). Note that we assumed strict genetic linkage between the mutations identified in a single-virus isolate, as the probability that it descended from a single infectious virion was > 0.9 (see above).

After grouping the virus isolates into genetic clusters, we tested whether the cluster had a significant effect on phenotype. We used generalized linear regressions with a beta error distribution (for survival and host clone range—the binomial distribution performed poorly due to complete separation; package "betareg," Cribari-Neto & Zeileis, 2010) or normal error distribution (for growth rate; package "lme4" Bates et al., 2015). Significance was tested using likelihood ratio tests and Tukey comparisons (package "multcomp," Hothorn et al., 2008). All analyses were done in R (R Core Team, 2020).

Fluctuating frequencies in the post-arms race phase

In both microcosms, the population-level host clone range fluctuated during the post-arms race phase (grey lines in Figure 2A). Since the population-level host clone range was determined using a fixed detection threshold (2,000 virions, time-shift experiment in Horas, 2022) and virus isolates differed in their host clone range (points in Figure 2A), we inferred that viral genotype frequencies fluctuated over time. For example, when the population-level host clone range was 1.0, genotypes with a host clone range of 1.0 must have been relatively common (cumulatively more than ~1 infectious virion/2,000 virions). At time points with lower population-level host clone ranges, genotypes with host clone range 1.0 must have been rare (fewer than ~1 infectious virion/2,000 virions).

Fortuitously, we were able to test the inference of fluctuating viral frequencies in microcosm I. In this microcosm, all isolates with host clone range > 0.3 (hereafter "intermediate-HCR") could infect algal clone A_I_34_5, but only those with host clone range > 0.7 (hereafter "high-HCR") could infect algal clone A_I_43_2 (Figure 1C). We used "most probable number" assays to measure the density of these phenotypes in the virus populations sampled from the coevolution experiment on days 67, 71, 76, 81, 85, and 90. Most probable number assays were done following Zimmerman (2017). For each virus population, 0.05 ml of a 10^{-2}, 10^{-3}, … , or 10^{-9}-diluted virus suspension was inoculated into 24 liquid culture wells containing A_I_34_5 or A_I_43_2, to a final volume of 0.2 ml and concentration of 2×10^5 algae/ml. The cultures were incubated for 6 days, after which wells were visually identified as virus-positive (lysed) or virus-negative. If necessary, incubation was extended for 2–4 more days. The most probable numbers of infectious virions capable of infecting A_I_34_5 (intermediate- and high-HCR infectious virions) and A_I_43_2 (high-HCR infectious virions) were calculated in R using the "MPN" package (Ferguson & Ihrie, 2019; R Core Team, 2020). The density of intermediate-HCR infectious virions was calculated by subtraction.

Experimental conditions

All assays described above were carried out in a liquid medium in cell culture flasks (algal growth and virus amplification) or 96-well cell culture plates (all other assays). We used Bold's Basal Medium (Nichols & Bold, 1965), with ammonium chloride substituted for sodium nitrate and double the concentration of trace element solution 4 (first used by Frickel et al., 2016). Flasks or culture plates were maintained at 20 °C, under constant light (40–45 µmol s^{-1} m^{-2}), and on an orbital shaker with a diameter of 10 mm and frequency of 120 rpm. Some culture plates were maintained without shaking in the final experiment (see above); this had no effect on the results. Algal cultures were generally in the late exponential to early stationary phase (1–4 × 10^6 algae/ml in this medium).

Downloaded from https://academic.oup.com/jeb/article/37/7/795/7663659 by Lib4RI - Library of Eawag, Empa, PSI, WSL user on 07 October 2024

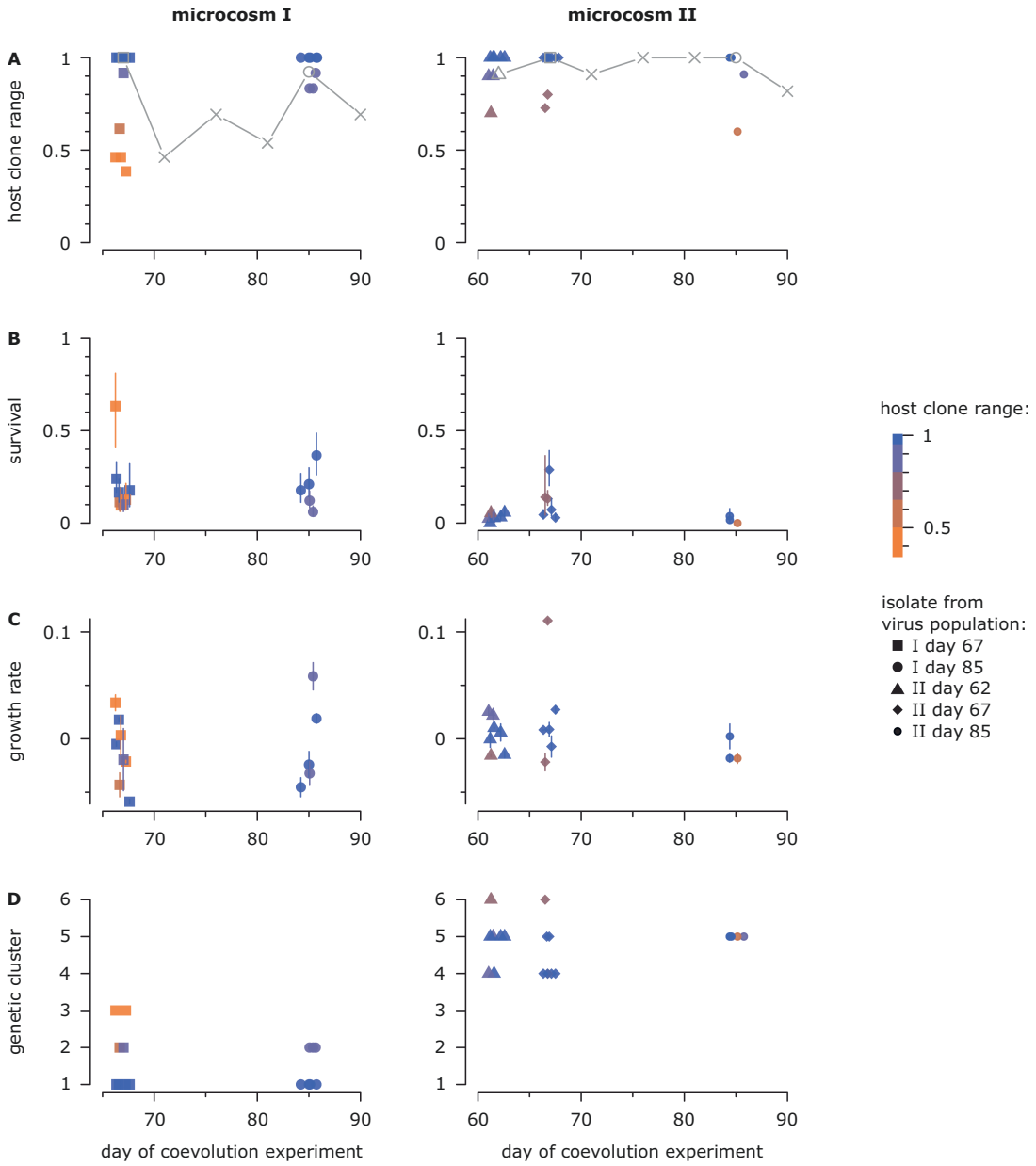


Figure 2. Virus diversity during the post-arms race phase. Points represent virus isolates; x-axis values are jittered. Virus isolates are coloured according to their host clone range; symbols group virus isolates from different populations. Note that not all virus isolates are represented in all panels (not all isolates were phenotyped and not all genotyping was successful, see Figure 1C and D). Phenotypic diversity is expressed as (A) the host clone range, (B) the proportion of infectious virions surviving after 7 days of exposure to 20 °C and constant light, and (C) the growth rate in the ancestor alga. Error bars represent the SEs of survival and growth rate across two replicates (SEs for survival not shown for the two virus isolates with 0 survival). In (A), the grey line represents the population-level host clone range when expressed on the same scale (i.e., proportion of the isolation algae + ancestor alga that could be infected). (D) Genetic diversity, expressed as the genetic cluster to which a virus isolate was assigned.

Results

Arms race confirmation

Using virus isolates obtained from the arms race and post-arms race phases, we confirmed that arms race dynamics had occurred. Virus isolates increased in host clone range over time (Figure 1C and D), and many post-arms race isolates were able to infect the same set of isolation algae as their source populations (Figure 2A, compare points to grey lines).

Diversity in the post-arms race phase

To assess viral diversity after the evolution of generalist-resistant algae, we focused on the viruses isolated from the beginning and end of the post-arms race phases (days 67 and 85 for microcosm I; days 62, 67, and 85 for microcosm II). We collected additional phenotypic and genotypic information for the majority of these isolates (marked under "P" and "G," Figure 1C and D).

In general, the virus isolates were phenotypically diverse throughout the post-arms race phase (Figure 2). Isolates with host clone range 1.0 and host clone range < 1.0 occurred at all time points, though in microcosm I the diversity was restricted on day 85 compared to day 67. Survival was diverse in microcosm I, but less so in microcosm II (particularly at time points 62 and 85). Although the growth rate in the ancestor alga was quantitatively diverse, qualitatively almost

Downloaded from https://academic.oup.com/jeb/article/37/7/795/7663659 by Lib4RI - Library of Eawag, Empa, PSI, WSL user on 07 October 2024

all isolates performed poorly (growth rate ~ 0). None of the phenotypes were significantly correlated ($p \geq 0.41$ after correction for multiple testing; Supplementary Figure S2).

As expected from their phenotypic diversity under standard conditions, the virus isolates were genetically diverse. The post-arms race isolates contained 19 loci with SNPs when compared to the ancestor virus (Supplementary Table S1). They also contained deletions between the positions 15 and 41 kb or 16 and 41 kb (Supplementary Table S1), a region which is regularly deleted in PBCV-1 (Landstein et al., 1995; Speciale et al., 2019). One isolate had low-quality sequences and was excluded from the analysis (marked under "G," Figure 1C). The post-arms race isolates belonged to six genetic clusters, which were separated by mutations at loci 65130 (gene A122/A123R), 65158 (gene A122/A123R), 254136 (gene A533R), and 259116 (gene A540L), and by the two deletions (Figure 3). Clusters 1–3 only occurred in microcosm I, with clusters 1 and 2 maintained throughout the post-arms race phase (Figure 2D). Clusters 4–6 were typical of microcosm II. All three clusters were detected at the beginning of the post-arms race phase, but only cluster 5 was detected at the end (Figure 2D).

The genetic diversity in the post-arms race phase isolates was associated with phenotypic variation in host clone range and survival (Figure 4). Clusters differed in their host clone range ($\chi^2(5) = 3.2$, $p < 0.001$), an effect driven by the significantly lower host clone range of clusters 2, 3, and 6 ($|z| \geq 4.1$, $p < 0.001$). Clusters also differed in survival ($\chi^2(5) = 2.6$, $p < 0.001$). The overall pattern was of lower survival in microcosm II: cluster 4 had significantly lower survival than clusters 1 and 3 ($|z| \geq 3.1$, $p \leq 0.02$), and cluster 5 had significantly lower survival than clusters 1, 2, and 3 ($|z| \geq 3.0$, $p \leq 0.03$). There was no effect of genetic cluster on the growth rate in the ancestor alga ($\chi^2(5) = -0.01$, $p = 0.20$).

Fluctuating frequencies in the post-arms race phase

Based on the fluctuating population-level host clone ranges (grey lines, Figure 2A) and diverse isolate-level host clone ranges (points, Figure 2A), we inferred that viral genotype frequencies fluctuated during the post-arms race phase (detailed explanation in *Methods*). We tested this inference in microcosm I by tracking the density of intermediate-HCR and high-HCR infectious viruses over the course of the post-arms race phase (host clone ranges 0.3–0.7 and > 0.7, respectively). We found that the densities of infectious intermediate-HCR and high-HCR virions fluctuated dramatically over time (Figure 5). The two phenotypes mostly replicated at different times: the high-HCR phenotype increased from days 71 to 76, the intermediate-HCR phenotype replicated from days 76 to 81 and 85 to 90, and both phenotypes increased from days 81 to 85. This is direct evidence of a dynamic polymorphism.

Discussion

We investigated the phenotypic and genetic diversity of the virus PBCV-1, after the end of its coevolutionary arms race with the unicellular alga *C. variabilis*—that is, after the evolution of generalist-resistant algae. Our results confirmed that the coevolution followed a transient arms race dynamic, and found that parasite diversity was maintained throughout the post-arms race phase. The isolates had variable genotypes and phenotypes and were particularly variable in their host clone range (Figure 2). Moreover, we showed that the host clone range followed a dynamic polymorphism in microcosm I (Figure 5). This work deepens our understanding of coevolution in the alga–virus system and in microbial communities in general.

Post-arms race polymorphisms

Our findings align with the theoretical expectation that host–parasite arms races can end in long-term host-range polymorphisms (Best et al., 2017; Brown & Tellier, 2011; Buckingham & Ashby, 2022). Experimental studies investigating this prediction are relatively scarce, as many coevolution experiments focus on the arms race phase or track only the parasite population. The available literature is dominated by bacteria-bacteriophage coevolution experiments. Not all bacteria-bacteriophage experiments with arms race dynamics led to the evolution of generalist-resistant hosts (Brockhurst et al., 2003; Buckling & Rainey, 2002) or maintained phage populations after the end of the arms race (Common et al., 2019). Of those that did, several found that host range diversity was maintained after the evolution of a generalist-resistant bacterium (Chao et al., 1977; Hall et al., 2011; Lopez Pascua et al., 2014; Marston et al., 2012), or that generalist-resistant bacteria coexisted with diverse phage phenotypes at the experimental end points (Poullain et al., 2008; Shaer Tamar & Kishony, 2022; Wandro et al., 2019 (with spatial structuring)). Combined with our results, it seems that the maintenance of post-arms race parasite diversity may be the norm in pro- and eukaryotic microbial systems. Since the evolution of generalist resistance and broad host range can be expected to be costly, this supports the overarching finding that coevolution is more likely to involve fluctuating selection dynamics as ecological "complications" increase (trade-offs, nutrient limitation, and spatial heterogeneity; Chao et al., 1977; Gómez & Buckling, 2011; Gómez et al., 2015; Lopez Pascua et al., 2014).

Although the post-arms race virus isolates were quite diverse (Figure 2), the true diversity of the virus populations must be even higher. We found that the isolate-based measurements underestimated host clone range diversity in microcosm I: although intermediate-HCR phenotypes were present on day 85 (Figure 5), these phenotypes were not represented among the virus isolates (Figure 2A). This is likely to be a sampling artefact: as we only used three isolation algae that could be infected by intermediate-HCR viruses, they were easily missed by chance. In microcosm II, there was "missing" genetic diversity: isolates 6.1, 45.1, 53.1, 79.2, 17.2, and 94.1 had the same unique genotype (cluster 4, Figure 3), but their host clone ranges varied between ~0.6 and 1.0 (Figure 1D). It is possible that the mutations conferring these host clone range phenotypes were not detected due to our stringent filtering process (compare Retel et al., 2019, 2022).

Trade-offs associated with expanding host (clone) range are some of the most powerful arguments explaining parasite diversity in general, and the end of arms race dynamics in particular (Brown & Tellier, 2011; Chao et al., 1977; Poullain et al., 2008). Although we did not find evidence for trade-offs in our post-arms race virus isolates, this may have been due to methodological limitations. In microcosm I, undersampling the intermediate-HCR isolates (see above) would have reduced our power to detect differences. To that end, it is interesting that the isolate with the highest survival in microcosm I had a narrow host clone range (Figure 2A). We also

Downloaded from https://academic.oup.com/jeb/article/37/7/795/7663659 by Lib4RI - Library of Eawag, Empa, PSI, WSL user on 07 October 2024

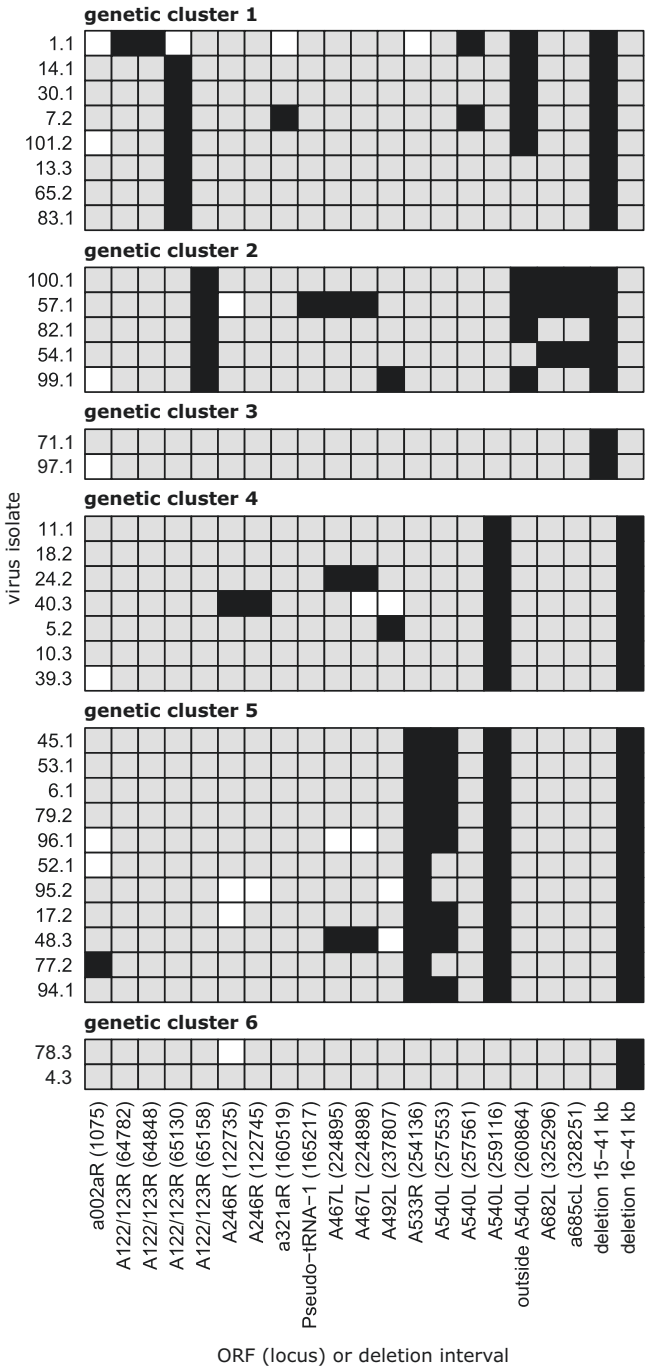


Figure 3. Composition of genetic clusters. Virus isolates are organized by their genetic cluster in order to visualize the characteristic mutations. Mutations are identified by ORF and locus (SNPs) or by interval (deletions). The genotyped virus isolates were identical to (grey) or different from (black) the ancestor virus genotype. White squares are NA. Names of the virus isolates are abbreviated from, e.g., "PBCV-1-H-13.3" to "13.3."

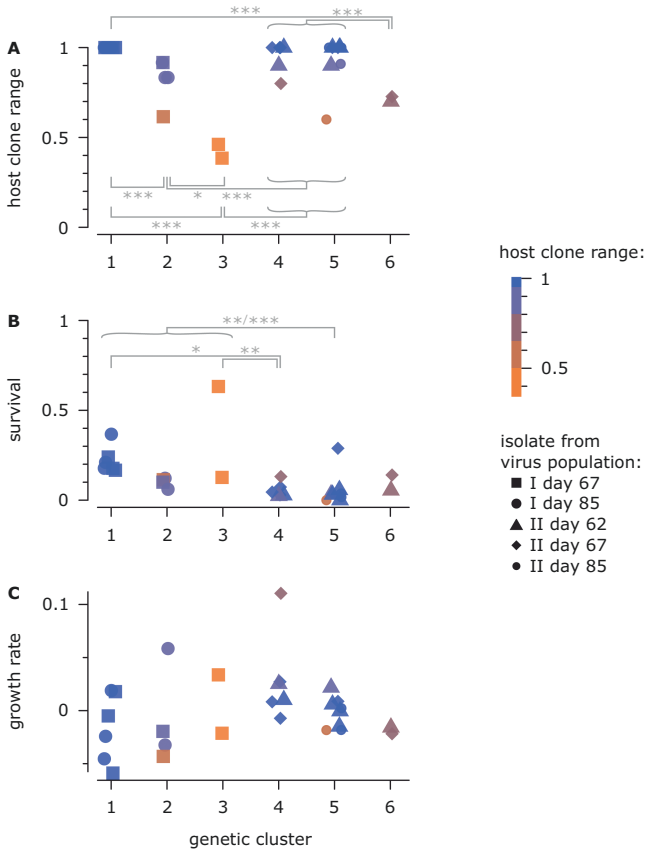


Figure 4. Genotype-phenotype association. Points represent virus isolates; x-axis values are jittered. Virus isolates are coloured according to their host clone range; symbols group virus isolates from different populations. Phenotypes are expressed as (A) the host clone range, (B) the proportion of infectious virions surviving after 7 days of exposure to 20 °C and constant light, and (C) the growth rate in the ancestor alga. The SEs of survival and growth rate are not represented here, as they were not taken into account in the statistics.

measured the isolates' growth in the ancestor alga instead of their contemporary host clones. Although this did reveal that expanding host clone range is associated with reduced fitness in the ancestor alga, this cost would not have been relevant during the post-arms race phase.

Mechanisms maintaining viral diversity in the post-arms race phase

Theory shows that long-term parasite polymorphisms can be maintained by selection for an equilibrium frequency, producing a static polymorphism, or by fluctuating selection, causing coevolutionary cycling (Best et al., 2017; Buckingham & Ashby, 2022; Woolhouse et al., 2002). The viral diversity at the beginning and end of the post-arms race phase (Figure 2) is compatible with either explanation, but the fluctuating population-level host clone ranges (Figure 2A) and fluctuating densities of intermediate-HCR and high-HCR viruses (Figure 5) indicate coevolutionary cycling.

It is clear that (semi-)susceptible algae were present during the post-arms race phase, since the intermediate-HCR and high-HCR viruses were actively growing (cf. Frickel et al., 2016; Retel et al., 2019). The population dynamics followed consumer-resource cycles, indicating that the density of (semi-)susceptible algae varied through time (Supplementary Figure S1; cycles cannot be caused by the unconsumable generalist-resistant algae). The maintenance of (semi-)susceptible algae, and thus of virus replication, was driven by a trade-off between algal resistance and growth (Horas, 2022).

Depending on the diversity of (semi-)susceptible algae, various selection mechanisms could have acted on the virus population. Two scenarios are possible given the data in Figure 5 (more details in Supplementary Figure S3): (a) The algal population contained a single (semi-)susceptible phenotype, susceptible to both intermediate- and high-HCR viruses, whose density fluctuated over time. If the host clone range was not costly, neither intermediate-HCR nor high-HCR viruses

Downloaded from https://academic.oup.com/jeb/article/37/7/795/7663659 by Lib4RI - Library of Eawag, Empa, PSI, WSL user on 07 October 2024

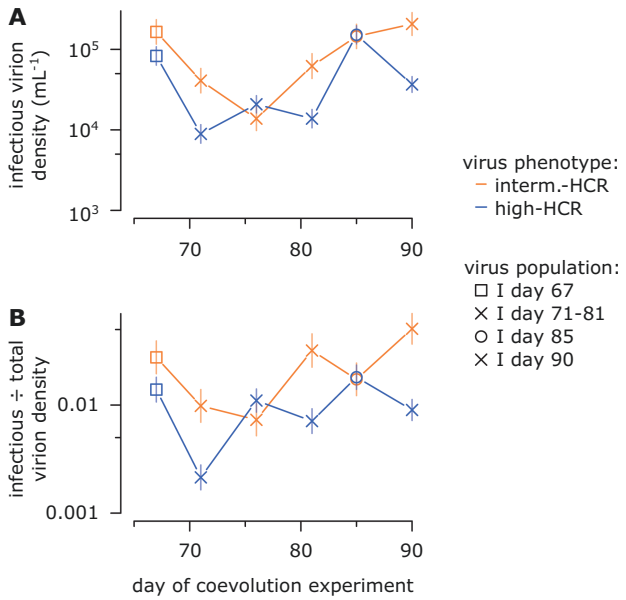


Figure 5. Density of virus phenotypes over the course of the post-arms race phase in microcosm I. Colors indicate intermediate- vs. high-HCR viruses; symbols follow Figure 2A. Both panels are on an *ln*-scale. (A) Density of the two phenotypes at each time point. Error bars represent the SE of the most probable number. (B) Frequencies of the two phenotypes (infectious virion density compared to the total virion density at that time point).

would be selected for, and a static polymorphism would be maintained. If the host clone range was costly, intermediate-HCR viruses would outcompete high-HCR viruses. (b) The algal population contained two or more (semi-)susceptible phenotypes, whose densities fluctuated over time: a phenotype susceptible to intermediate- and high-HCR viruses, and a phenotype susceptible to high-HCR viruses. In a population without extinction where the host clone range was not costly, fluctuations between the two algal phenotypes would be sufficient to maintain the viral polymorphism (Frickel et al., 2016). More realistically, high-HCR viruses would likely outcompete intermediate-HCR viruses, as they would be selected for when the second algal phenotype dominated. If the host clone range traded off with growth or survival, high-HCR viruses would be selected for when the second algal phenotype was present, but not at other times. Thus fluctuating selection could maintain a dynamic viral polymorphism (coevolutionary cycling or "range FSD"; Best et al., 2017; Hall et al., 2011; Lopez Pascua et al., 2014).

In a deterministic world, therefore, the cyclical polymorphism in microcosm I (Figure 5) would be proof of fluctuating selection for (costly) host clone range (scenario B with costs of host clone range). However, viruses are highly susceptible to demographic stochasticity (Gillespie, 1998; Irwin et al., 2016). Viruses have highly skewed reproductive distributions (~1,500 new virions per successful infection for PBCV-1, Lievens et al., 2023), and rely on random chance to encounter host cells. When algal densities are low, host encounters are rare. For example, we estimate that ~10 infectious high-HCR virions would encounter an algal cell within 24 hr on day 71 (adsorption constant conservatively estimated at 5×10^{-10}, E.J.P. Lievens unpublished data, smoothed algal density ~1,750 algae/ml, high-HCR density ~9,000 infectious virions/ml, time 1,440 min; Hyman & Abedon, 2009, eq. 18.2). Thus stochasticity in the order of host encounter, magnified by the large number of offspring, could obscure any fitness differences between intermediate-HCR and high-HCR viruses. This could lead to dynamic polymorphisms in the absence of fluctuating selection (more details in Supplementary Figure S3, cf. Lopez Pascua et al., 2014). Following the calculation above, we expect that stochasticity played a larger role around days 71–76 (~10–50 infectious virions expected to encounter a host cell within 24 hr), which could explain why only intermediate-HCR viruses replicated between days 76 and 81 (algae susceptible to intermediate-HCR viruses were also susceptible to high-HCR viruses). At time points with larger virus and algal populations, however, we expect fitness differences to be more important than stochasticity (e.g., days 67, 81, 85, and 90: ~250–2,500 infectious virions of each phenotype expected to encounter a host cell within 24 hr).

Overall, we hypothesize that the (co)evolutionary cycling observed in microcosm I was caused by a combination of fluctuating selection for host clone range and demographic stochasticity. Microcosm II and the similar microcosms in Retel et al. (2019) also saw dramatic fluctuations in the size of algal and viral populations during the post-arms race phase (data not shown), so we expect the same mechanisms to have been at play. Theory predicts that stochasticity can reduce or increase polymorphism in host–parasite coevolution, depending on the model details (Brown & Tellier, 2011; Gokhale et al., 2013; Kirby & Burdon, 1997), so theoretical models that explicitly consider virus biology would be particularly welcome. Such models could test our intuitive expectations, explore the population densities at which stochasticity becomes important, and examine the persistence of stochasticity-driven polymorphisms.

Genetics of host clone range evolution

Roughly half of the SNPs we detected in the post-arms race phase were in genes that mutated in a previous *Chlorella*-virus coevolution experiment (Supplementary Table S2; Retel et al., 2019, 2022). Gene A122/123R codes for a minor capsid "fibre" protein (Shao et al., 2022), which may help attach the virion to the host cell (Van Etten et al., 1991). Gene A533R produces the 'penton' protein that surrounds the virion's spike structure, through which viral DNA enters the host cell (Milrot et al., 2017; Shao et al., 2022). Genes A246 and A540L are virion-associated proteins with unknown functions. However, both are members of "gene gangs" (genes in close proximity whose functions are expected to be related, Seitzer et al., 2018), which suggests that their functions are important and relatively conserved. Gene A540L is in the same gene gang as A533R, so its function may also be infection-related (Retel et al., 2022; Seitzer et al., 2018). The deletions between 15 and 41 or 16 and 41 kb, which occurred in all post-arms race isolates, also encompass genes associated with *Chlorella*-virus coevolution (Retel et al., 2019, 2022). Of particular interest are gene A025/027/029L (16.4–20.5 kb), which also encodes a minor capsid "fiber" protein (Shao et al., 2022), and gene A064R, which glycosylates the major capsid protein (Speciale et al., 2019). Overall the mutated genes seem to be associated with the processes of attachment and DNA entry, consistent with the observation that *Chlorella* resistance usually manifests through attachment (Quispe et al., 2017; Yamada et al., 2006).

Interestingly, different mutations dominated in microcosms I and II (Figure 3). Mutations in gene A122/123R were

Downloaded from https://academic.oup.com/jeb/article/37/7/795/7663659 by Lib4RI - Library of Eawag, Empa, PSI, WSL user on 07 October 2024

characteristic of microcosm I, but not detected in microcosm II. Conversely, mutations in A533R and A540L were characteristic of microcosm II (only two isolates in microcosm I had mutations in these genes, at a locus of A540L that was absent in microcosm II). This finding could be explained by historical contingency—for example, if the SNP at locus 259116 was fixed early on in microcosm II—, but previous work found that PBCV-1 is not mutation-limited in microcosm experiments (Retel et al., 2022). In this case, it should have been possible for the virus populations to explore all allele combinations. The pattern is unlikely to be an artefact caused by repeated sampling of the same genotypes, as the lack of overlap is significant when considering only unique genotypes (n = 7, 8, and 2 genotypes with mutations in, respectively, A122/123R, A540L, and both; $\chi^2(1) = 7.6$, $p = 0.01$). Instead, potential explanations include: (a) The algal resistance phenotypes in microcosms I and II required different counter-adaptations. This is somewhat supported by previous work, which found that algal populations from different microcosms did not share any high-frequency mutations (Frickel et al., 2018; Retel et al., 2019). However, this may not have affected the algal phenotypes: Frickel et al. (2016) also found that viruses from different microcosms were cross-infective, and this was also true of virus isolates from day 34 of microcosms I and II (S. Kühn, data not shown). (b) Strong drift counteracted the diversifying effects of mutation supply, e.g., due to the virus' highly differential reproductive success (Lievens et al., 2023). (c) Mutations at the two sites have negative epistatic interactions (Bedhomme et al., 2015; Zhao et al., 2019). Epistasis would need to be site-specific, as previous work found that mutations at different loci in genes A540L and A122/123R can co-occur (Retel et al., 2019). Negative epistasis may also occur between loci 65130 and 65158, since no isolates were found with both derived alleles in microcosm I ($\chi^2(1) = 4.3$, $p = 0.04$; Figure 3).

Conclusion

Although experimental coevolution in microbial host–parasite systems often follows arms race dynamics, these arms races are usually finite. The post-arms race phase is likely to be more representative of natural conditions (Brown & Tellier, 2011; Flores et al., 2011; Hall et al., 2011; Poisot et al., 2013), so understanding its development is a bridge to interpreting natural host–parasite systems. We have shown that in experimental alga–virus coevolutions, virus populations maintained considerable diversity after the end of the arms race. Viral host clone range phenotypes fluctuated in frequency, suggesting a role for fluctuating selection in the maintenance of diversity. Our results align with studies of experimental coevolution between bacteria and bacteriophage (Chao et al., 1977; Hall et al., 2011; Lopez Pascua et al., 2014; Marston et al., 2012; Poullain et al., 2008; Shaer Tamar & Kishony, 2022; Wandro et al., 2019), and suggest that the maintenance of parasite diversity is common across microbial systems.

Supplementary material

Supplementary material is available at *Journal of Evolutionary Biology* online.

Data availability

Raw phenotypic data, processed phenotypic data, processed genetic data, and analysis scripts are available on Zenodo at https://zenodo.org/doi/10.5281/zenodo.10715678. Viral sequences are available in the European Nucleotide Archive (ENA) at EMBL-EBI under accession number PRJEB72687 (https://www.ebi.ac.uk/ena/browser/view/PRJEB72687).

Author contributions

Eva Lievens (Conceptualization, Data curation, Formal analysis, Investigation, Methodology, Supervision, Writing—original draft, Writing—review & editing), Samuel Kühn (Data curation, Formal analysis, Investigation, Methodology, Writing—review & editing), Elena Horas (Conceptualization, Resources, Writing—review & editing), Guénolé Le Pennec (Data curation, Formal analysis, Writing—review & editing), Sarah Peter (Investigation), Azade Petrosky (Investigation), Sven Künzel (Investigation), Philine Feulner (Data curation, Funding acquisition, Writing—review & editing), and Lutz Becks (Conceptualization, Funding acquisition, Resources, Supervision)

Funding

This work was supported by the German Research Foundation (DFG) to L.B. (grants BE 4135/8-1, BE 4135/5-2), and by the Swiss National Science Foundation (SNSF) to P.G.D.F. (grant 310030E_179637); E.H. was supported by the International Max Planck Research School for Organismal Biology. Genomic data analysis was supported by collaboration with the Genetic Diversity Centre (GDC), ETH Zürich.

Acknowledgments

We thank the team at the Max Planck Institute sequencing centre in Plön for carrying out the DNA sequencing, T. Häring for help with the time-shift experiment, and M. Spagnuolo for help with the DNA extractions. We acknowledge the Flow Cytometry Centre (FlowKon) at the University of Konstanz for the use of flow cytometers and the expert support in instrument usage and data analysis. Finally, we thank the editor I. Bravo for his helpful comments on the bioinformatic analyses.

Conflict of interest

None declared.

References

Agrawal, A., & Lively, C. M. (2002). Infection genetics: Gene-for-gene versus matching-alleles models and all points in between. *Evolutionary Ecology Research*, *4*, 79–90.

Bates, D., Maechler, M., Bolker, B., & Walker, S. (2015). Fitting linear mixed-effects models using lme4. *Journal of Statistical Software*, *67*, 1–48. https://doi.org/10.18637/jss.v067.i01

Bedhomme, S., Hillung, J., & Elena, S. F. (2015). Emerging viruses: Why they are not jacks of all trades? *Current Opinion in Virology*, *10*, 1–6. https://doi.org/10.1016/j.coviro.2014.10.006

Best, A., Ashby, B., White, A., … Boots, M. (2017). Host–parasite fluctuating selection in the absence of specificity. *Proceedings of the Royal Society of London, Series B: Biological Sciences*, *284*(1866), 20171615. https://doi.org/10.1098/rspb.2017.1615

Brockhurst, M. A., Morgan, A. D., Rainey, P. B., & Buckling, A. (2003). Population mixing accelerates coevolution. *Ecology Letters*, *6*(11), 975–979. https://doi.org/10.1046/j.1461-0248.2003.00531.x

Downloaded from https://academic.oup.com/jeb/article/37/7/795/7663659 by Lib4RI - Library of Eawag, Empa, PSI, WSL user on 07 October 2024

Brown, J. K. M., & Tellier, A. (2011). Plant-parasite coevolution: Bridging the gap between genetics and ecology. *Annual Review of Phytopathology*, *49*(1), 345–367. https://doi.org/10.1146/annurev-phyto-072910-095301

Buckingham, L. J., & Ashby, B. (2022). Coevolutionary theory of hosts and parasites. *Journal of Evolutionary Biology*, *35*(2), 205–224. https://doi.org/10.1111/jeb.13981

Buckling, A., & Rainey, P. B. (2002). Antagonistic coevolution between a bacterium and a bacteriophage. *Proceedings of the Royal Society of London, Series B: Biological Sciences*, *269*(1494), 931–936. https://doi.org/10.1098/rspb.2001.1945

Chao, L., Levin, B. R., & Stewart, F. M. (1977). A complex community in a simple habitat: An experimental study with bacteria and phage. *Ecology*, *58*(2), 369–378. https://doi.org/10.2307/1935611

Chen, S., Zhou, Y., Chen, Y., & Gu, J. (2018). fastp: An ultra-fast all-in-one FASTQ preprocessor. *Bioinformatics*, *34*(17), i884–i890. https://doi.org/10.1093/bioinformatics/bty560

Cingolani, P., Platts, A., Wang, L. L., ... Ruden, D. M. (2012). A program for annotating and predicting the effects of single nucleotide polymorphisms, SnpEff. *Fly*, *6*(2), 80–92. https://doi.org/10.4161/fly.19695

Clarke, B. C. (1979). The evolution of genetic diversity. *Proceedings of the Royal Society of London, Series B, Biological Sciences*, *205*(1161), 453–474. https://doi.org/10.1098/rspb.1979.0079

Common, J., Morley, D., Westra, E. R., & van Houte, S. (2019). CRISPR-Cas immunity leads to a coevolutionary arms race between *Streptococcus thermophilus* and lytic phage. *Philosophical Transactions of the Royal Society of London, Series B: Biological Sciences*, *374*(1772), 20180098. https://doi.org/10.1098/rstb.2018.0098

Cribari-Neto, F., & Zeileis, A. (2010). Beta regression in R. *Journal of Statistical Software*, *34*(2), 1–24. https://doi.org/10.18637/jss.v034.i02

Danecek, P., Auton, A., Abecasis, G., … Durbin, R.; 1000 Genomes Project Analysis Group. (2011). The variant call format and VCFtools. *Bioinformatics*, *27*, 2156–2158. https://doi.org/10.1093%2Fbioinformatics%2Fbtr330

Ferguson, M., & Ihrie, J. (2019). *MPN: Most probable number and other microbial enumeration techniques*. R package version 0.3.0. https://CRAN.R-project.org/package=MPN

Flores, C. O., Meyer, J. R., Valverde, S., … Weitz, J. S. (2011). Statistical structure of host–phage interactions. *Proceedings of the National Academy of Sciences of the United States of America*, *108*(28), E288–E297. https://doi.org/10.1073/pnas.1101595108

Frickel, J., Feulner, P. G. D., Karakoc, E., & Becks, L. (2018). Population size changes and selection drive patterns of parallel evolution in a host–virus system. *Nature Communications*, *9*(1), 1706. https://doi.org/10.1038/s41467-018-03990-7

Frickel, J., Sieber, M., & Becks, L. (2016). Eco-evolutionary dynamics in a co-evolving host-virus system. *Ecology Letters*, *19*(4), 450–459. https://doi.org/10.1111/ele.12580

Genolini, C., Alacoque, X., Sentenac, M., & Arnaud, C. (2015). kml and kml3d: R Packages to cluster longitudinal data. *Journal of Statistical Software*, *65*(4), 1–34. https://doi.org/10.18637/jss.v065.i04

Gillespie, J. H. (1998). *Population genetics: A concise guide* (2nd ed.). John Hopkins University Press.

Gokhale, C. S., Papkou, A., Traulsen, A., & Schulenburg, H. (2013). Lotka–Volterra dynamics kills the Red Queen: Population size fluctuations and associated stochasticity dramatically change host-parasite coevolution. *BMC Evolutionary Biology*, *13*, 254. https://doi.org/10.1186/1471-2148-13-254

Gómez, P., Ashby, B., & Buckling, A. (2015). Population mixing promotes arms race host–parasite coevolution. *Proceedings of the Royal Society of London, Series B: Biological Sciences*, *282*(1798), 20142297. https://doi.org/10.1098/rspb.2014.2297

Gómez, P., & Buckling, A. (2011). Bacteria-phage antagonistic coevolution in soil. *Science*, *332*(6025), 106–109. https://doi.org/10.1126/science.1198767

Gower, J. C. (1971). A general coefficient of similarity and some of its properties. *Biometrics*, *27*(4), 857–874. https://doi.org/10.2307/2528823

Hall, A. R., Scanlan, P. D., Morgan, A. D., & Buckling, A. (2011). Host-parasite coevolutionary arms races give way to fluctuating selection. *Ecology Letters*, *14*(7), 635–642. https://doi.org/10.1111/j.1461-0248.2011.01624.x

Holm, S. (1979). A simple sequentially rejective multiple test procedure. *Scandinavian Journal of Statistics*, *6*, 65–70.

Horas, E. L. (2022). *The effects of symbiotic interactions on the ecology and evolution of the alga Chlorella variabilis*. University of Konstanz.

Hothorn, T., Bretz, F., & Westfall, P. (2008). Simultaneous inference in general parametric models. *Biometrical Journal*, *50*(3), 346–363. https://doi.org/10.1002/bimj.200810425

Hyman, P., & Abedon, S. T. (2009). Practical methods for determining phage growth parameters. In M. R. J. Clokie, & A. M. Kropinski (Eds.), *Bacteriophages: Methods and protocols, Volume 1: Isolation, characterization, and interactions* (Vol. *401*, pp. 175–202). Humana Press. https://doi.org/10.1007/978-1-60327-164-6_18

Irwin, K. K., Laurent, S., Matuszewski, S., … Jensen, J. D. (2016). On the importance of skewed offspring distributions and background selection in virus population genetics. *Heredity*, *117*(6), 393–399. https://doi.org/10.1038/hdy.2016.58

Kashiwagi, A., & Yomo, T. (2011). Ongoing phenotypic and genomic changes in experimental coevolution of RNA bacteriophage Qβ and *Escherichia coli*. *PLoS Genetics*, *7*(8), e1002188. https://doi.org/10.1371/journal.pgen.1002188

Kaufman, L., & Rousseeuw, P. J. (1990). Partitioning around medoids (Program PAM). In *Finding groups in data: An introduction to cluster analysis*. John Wiley & Sons. https://doi.org/10.1002/9780470316801.ch2

Kirby, G. C., & Burdon, J. J. (1997). Effects of mutation and random drift on Leonard's gene-for-gene coevolution model. *Phytopathology*, *87*(5), 488–493. https://doi.org/10.1094/PHYTO.1997.87.5.488

Landstein, D., Burbank, D. E., Nietfeldt, J. W., & Van Etten, J. L. (1995). Large deletions in antigenic variants of the chlorella virus PBCV-1. *Virology*, *214*(2), 413–420. https://doi.org/10.1006/viro.1995.0051

Larsen, M. L., Wilhelm, S. W., & Lennon, J. T. (2019). Nutrient stoichiometry shapes microbial coevolution. *Ecology Letters*, *22*(6), 1009–1018. https://doi.org/10.1111/ele.13252

Lenski, R. E. (1984). Coevolution of bacteria and phage: Are there endless cycles of bacterial defenses and phage counterdefenses? *Journal of Theoretical Biology*, *108*(3), 319–325. https://doi.org/10.1016/s0022-5193(84)80035-1

Lenski, R. E., & Levin, B. R. (1985). Constraints on the coevolution of bacteria and virulent phage: A model, some experiments, and predictions for natural communities. *The American Naturalist*, *125*(4), 585–602. https://doi.org/10.1086/284364

Li, H., & Durbin, R. (2009). Fast and accurate short read alignment with Burrows–Wheeler transform. *Bioinformatics*, *25*(14), 1754–1760. https://doi.org/10.1093/bioinformatics/btp324

Lievens, E. J. P. (2023). *Modified survival (mS) assay*. https://dx.doi.org/10.17504/protocols.io.81wgb6knylpk/v3

Lievens, E. J. P. (2022). *Virion quantification by flow cytometry, without fixation or freezing*. https://dx.doi.org/10.17504/protocols.io.6qpvr6q93vmk/v1

Lievens, E. J. P., Agarkova, I. V., Dunigan, D. D., … Becks, L. (2023). Efficient assays to quantify the life history traits of algal viruses. *Applied and Environmental Microbiology*, *89*(12), e0165923. https://doi.org/10.1128/aem.01659-23

Lopez Pascua, L., Hall, A. R., Best, A., … Buckling, A. (2014). Higher resources decrease fluctuating selection during host–parasite coevolution. *Ecology Letters*, *17*(11), 1380–1388. https://doi.org/10.1111/ele.12337

Maechler, M., Rousseeuw, P., Struyf, A., … Hornik, K. (2022). *cluster: Cluster analysis basics and extensions*. R package version 2.1.4. https://CRAN.R-project.org/package=cluster

Marston, M. F., Pierciey, F. J., Shepard, A., … Martiny, J. B. H. (2012). Rapid diversification of coevolving marine *Synechococcus* and a virus. *Proceedings of the National Academy of Sciences of*

Downloaded from https://academic.oup.com/jeb/article/37/7/795/7663659 by Lib4RI - Library of Eawag, Empa, PSI, WSL user on 07 October 2024

the United States of America, *109*(12), 4544–4549. https://doi.org/10.1073/pnas.1120310109

Milrot, E., Shimoni, E., Dadosh, T., … Minsky, A. (2017). Structural studies demonstrating a bacteriophage-like replication cycle of the eukaryote-infecting *Paramecium bursaria* chlorella virus-1. *PLoS Pathogens*, *13*(8), e1006562. https://doi.org/10.1371/journal.ppat.1006562

Mizoguchi, K., Morita, M., Fischer, C. R., … Unno, H. (2003). Coevolution of bacteriophage PP01 and *Escherichia coli* O157:H7 in continuous culture. *Applied and Environmental Microbiology*, *69*(1), 170–176. https://doi.org/10.1128/AEM.69.1.170-176.2003

Nichols, H. W., & Bold, H. C. (1965). *Trichosarcina polymorpha* Gen. et Sp. Nov. *Journal of Phycology*, *1*(1), 34–38. https://doi.org/10.1111/j.1529-8817.1965.tb04552.x

Perry, E. B., Barrick, J. E., & Bohannan, B. J. M. (2015). The molecular and genetic basis of repeatable coevolution between *Escherichia coli* and bacteriophage T3 in a laboratory microcosm. *PLoS One*, *10*(6), e0130639. https://doi.org/10.1371/journal.pone.0130639

Picelli, S., Björklund, A. K., Reinius, B., … Sandberg, R. (2014). Tn5 transposase and tagmentation procedures for massively scaled sequencing projects. *Genome Research*, *24*(12), 2033–2040. https://doi.org/10.1101/gr.177881.114

Poisot, T., Lounnas, M., & Hochberg, M. E. (2013). The structure of natural microbial enemy-victim networks. *Ecological Processes*, *2*(1), 13. https://doi.org/10.1186/2192-1709-2-13

Poullain, V., Gandon, S., Brockhurst, M. A., … Hochberg, M. E. (2008). The evolution of specificity in evolving and coevolving antagonistic interactions between a bacteria and its phage. *Evolution*, *62*(1), 1–11. https://doi.org/10.1111/j.1558-5646.2007.00260.x

Quispe, C. F., Esmael, A., Sonderman, O., … Van Etten, J. L. (2017). Characterization of a new *Chlorovirus* type with permissive and non-permissive features on phylogenetically related algal strains. *Virology*, *500*, 103–113. https://doi.org/10.1016/j.virol.2016.10.013

R Core Team. (2020). *R: A language and environment for statistical computing*. R Foundation for Statistical Computing.

Retel, C., Kowallik, V., Becks, L., & Feulner, P. G. D. (2022). Strong selection and high mutation supply characterize experimental *Chlorovirus* evolution. *Virus Evolution*, *8*(1), veac003. https://doi.org/10.1093/ve/veac003

Retel, C., Kowallik, V., Huang, W., … Feulner, P. G. D. (2019). The feedback between selection and demography shapes genomic diversity during coevolution. *Science Advances*, *5*(10), eaax0530. https://doi.org/10.1126/sciadv.aax0530

Scrucca, L., Fop, M., Murphy Brendan, T., & Raftery E, A. (2016). mclust 5: Clustering, classification and density estimation using Gaussian finite mixture models. *The R Journal*, *8*, 289–317.

Seitzer, P., Jeanniard, A., Ma, F., … Dunigan, D. D. (2018). Gene gangs of the chloroviruses: Conserved clusters of collinear monocistronic genes. *Viruses*, *10*(10), 576. https://doi.org/10.3390/v10100576

Shaer Tamar, E., & Kishony, R. (2022). Multistep diversification in spatiotemporal bacterial-phage coevolution. *Nature Communications*, *13*(1), 7971. https://doi.org/10.1038/s41467-022-35351-w

Shao, Q., Agarkova, I. V., Noel, E. A., … Fang, Q. (2022). Near-atomic, non-icosahedrally averaged structure of giant virus *Paramecium bursaria* chlorella virus 1. *Nature Communications*, *13*(1), 6476. https://doi.org/10.1038/s41467-022-34218-4

Speciale, I., Duncan, G. A., Unione, L., … De Castro, C. (2019). The N-glycan structures of the antigenic variants of chlorovirus PBCV-1 major capsid protein help to identify the virus-encoded glycosyltransferases. *The Journal of Biological Chemistry*, *294*(14), 5688–5699. https://doi.org/10.1074/jbc.RA118.007182

Swihart, B., & Lindsey, J. (2022). *repeated: Non-normal repeated measurements models*. R package version 1.1.6. https://CRAN.R-project.org/package=repeated

Tam, E. (2022). *Kneedle algorithm in R—Detecting knees in graphs*. https://github.com/etam4260/kneedle?tab=readme-ov-file

Van der Auwera, G. A., & O'Connor, B. D. (2020). *Genomics in the cloud*. O'Reilly Media.

Van Etten, J. L., Agarkova, I. V., & Dunigan, D. D. (2020). Chloroviruses. *Viruses*, *12*(1), 20. https://doi.org/10.3390/v12010020

Van Etten, J. L., Burbank, D. E., Kuczmarski, D., & Meints, R. H. (1983a). Virus infection of culturable *Chlorella*-like algae and development of a plaque assay. *Science*, *219*(4587), 994–996. https://doi.org/10.1126/science.219.4587.994

Van Etten, J. L., Burbank, D. E., Xia, Y., & Meints, R. H. (1983b). Growth cycle of a virus, PBCV-1, that infects *Chlorella*-like algae. *Virology*, *126*(1), 117–125. https://doi.org/10.1016/0042-6822(83)90466-x

Van Etten, J. L., Lane, L. C., & Meints, R. H. (1991). Viruses and virus-like particles of eukaryotic algae. *Microbiological Reviews*, *55*(4), 586–620. https://doi.org/10.1128/mr.55.4.586-620.1991

Wandro, S., Oliver, A., Gallagher, T., … Whiteson, K. (2019). Predictable molecular adaptation of coevolving *Enterococcus faecium* and lytic phage EfV12-phi1. *Frontiers in Microbiology*, *9*, 3192. https://doi.org/10.3389/fmicb.2018.03192

Woolhouse, M. E. J., Webster, J. P., Domingo, E., … Levin, B. R. (2002). Biological and biomedical implications of the co-evolution of pathogens and their hosts. *Nature Genetics*, *32*(4), 569–577. https://doi.org/10.1038/ng1202-569

Yamada, T., Onimatsu, H., & Van Etten, J. L. (2006). *Chlorella* viruses. *Advances in Virus Research*, *66*, 293–336. https://doi.org/10.1016/S0065-3527(06)66006-5

Zhao, L., Seth-Pasricha, M., Stemate, D., … Duffy, S. (2019). Existing host range mutations constrain further emergence of RNA viruses. *Journal of Virology*, *93*(4), e01385. https://doi.org/10.1128/JVI.01385-18

Zimmerman, A. (2017). *MPN (Most Probable Number) assay for infectivity of algal viruses*. https://dx.doi.org/10.17504/protocols.io.gunbwve

Downloaded from https://academic.oup.com/jeb/article/37/7/795/7663659 by Lib4RI - Library of Eawag, Empa, PSI, WSL user on 07 October 2024